COMMUNICATION

Electrofocusing-enhanced localized surface plasmon resonance biosensors†

Jinling Zhang,‡[a] Yi Wang,‡[a] Ten It Wong,[b] Xiaohu Liu,[a] Xiaodong Zhou[b] and Bo Liedberg*[a]

Localized surface plasmon resonance (LSPR) biosensors typically suffer from diffusion limited mass transport and nonspecific adsorption upon detection of biomolecules in real biofluids. We employ here a peptide-modified plasmonic gold nanohole (AuNH) array for real-time detection of human troponin I (cTnI). Applying a negative electric bias on the AuNH sensor chip enables us to attract and concentrate cTnI at the sensor surface, while repelling other proteins thus decreasing interferences due to nonspecific adsorption.

Surface plasmon resonance (SPR) originates from collective oscillations of the free electron cloud in metals.[1] Due to the high field enhancement and high sensitivity of SPR to the refractive index changes, it has been extensively applied in photo-catalysis,[2–4] opto-electronic devices[5] and biosensors[6–8] based on label-free,[4,9–11] fluorescence enhancement[12–16] and surface enhanced Raman scattering.[17–20] Label-free SPR biosensors typically provide a limit of detection (LOD) in the 0.1–10 ng cm^{-2} regime.[6] There are several key factors limiting the sensitivity of SPR sensors, including (1) the bulk refractive index sensitivity of SPR, (2) the diffusion limited mass transport of the target molecules to the sensor surface which slows down the molecular binding and limits the sensor response, and (3) the high nonspecific adsorption of undesirable molecules on the sensor surface such as albumin in serum samples which might lead to erroneous responses *e.g.* due to blocking of specific binding sites. Several methods have been employed to boost the sensitivity including well-designed nanostructures with improved refractive-index sensitivity,[11] amplification of the SPR signal with nanoparticles[21–24] and enzyme labeling,[25,26] tuning the pH of samples to minimize the nonspecific

adsorption,[27] and applying magnetic field[28,29] and electric field[30–33] to promote molecular diffusion. For instance, magnetic fields enabled rapid capture of magnetic nanoparticle-targeted hCG and *E. coli* bacteria to a grating-coupled SPR sensor surface.[28,29] In addition, the electric field applied to a LSPR sensor chip offered a route to control the adsorption of molecules to the sensor surface.[32,33] Furthermore, the influences of the applied electric field on the SPR response have been discussed,[34–39] and several groups integrated electric biasing or electrochemistry with LSPR for biosensing.[32,40,41] However, limited research has been devoted to studies aiming at reducing the nonspecific adsorption of abundant molecules such as serum albumin, an important plasma protein, while enhancing the binding of target molecules to the sensor surface.

Here, we present a combined LSPR electrofocusing platform for the detection of human troponin I (cTnI), a biomarker of myocardial infarction. A gold nanohole (AuNH) array is employed both as the LSPR sensor chip and as the working electrode. The LSPR sensor responses upon the binding of cTnI and the nonspecific adsorption of bovine serum albumin (BSA) were investigated on the AuNH substrate under different biases. As the isoelectric point of cTnI (pI = 9.87) is higher than for BSA (pI = 4.7), a negative bias applied on the sensor surface is expected to favour the specific capture of cTnI while repelling BSA molecules from the sensor surface (Fig. 1a). In addition, the bias applied on the substrate creates a high electric field gradient at the edge of the nanohole, thereby offering an efficient means of capturing molecules at the edge of the nanoholes where the plasmon field provides the highest sensitivity to refractive index changes.[42] Therefore, the sensitivity for selective detection of cTnI is expected to improve significantly under negative biases applied on the sensor chip.

The AuNH array was prepared through a series of steps involving nickel mold fabrication by electron beam lithography (EBL) and AuNH array production by nano-imprinting (see experimental details in the ESI†).[43,44] An area of 2 × 2 mm^2 consisting of a layer of 50 nm Au coated on glass with periodic (pitch of 400 nm) holes of 140 nm in diameter is located at

[a]Centre for Biomimetic Sensor Science, School of Materials Science and Engineering, Nanyang Technological University, 50 Nanyang Drive, Singapore 637553. E-mail: bliedberg@ntu.edu.sg, yiwang@ntu.edu.sg
[b]Institute of Materials Research and Engineering, Agency for Science, Technology and Research (A*STAR), 3 Research Link, Singapore 117602
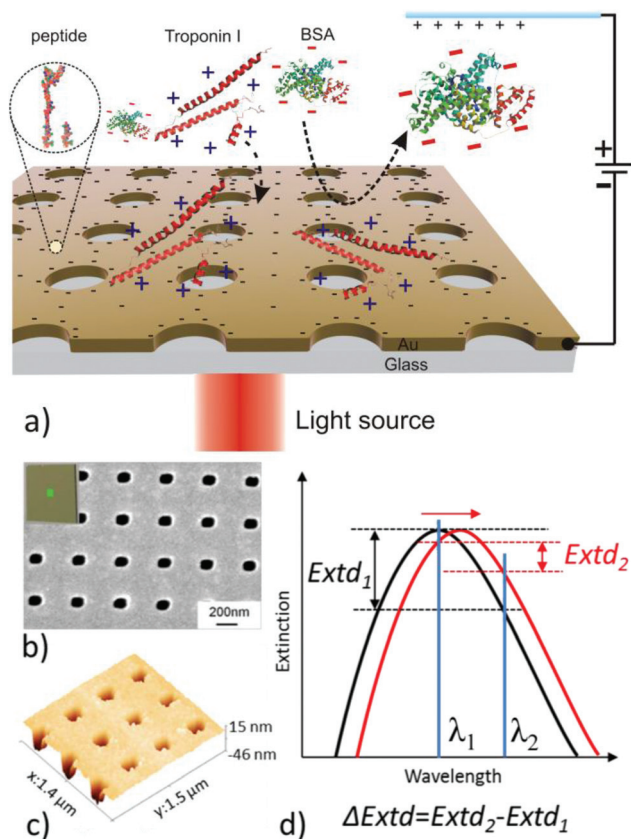
Fig. 1 (a) Schematic illustration of the setup and the modified AuNH array chip applied with a negative bias for minimizing the nonspecific adsorption of BSA and simultaneously attracting the target cTnI to the sensor surface. (b) SEM and a photo of the chip (inset). (c) AFM image of AuNH array. (d) The extinction spectra of AuNH array typically shift to a longer wavelength upon molecular binding, leading to decrease of the extinction difference Extd derived from two preselected wavelengths λ_1 and λ_2. The change of Extd is defined as ΔExtd = Extd$_2$ − Extd$_1$.
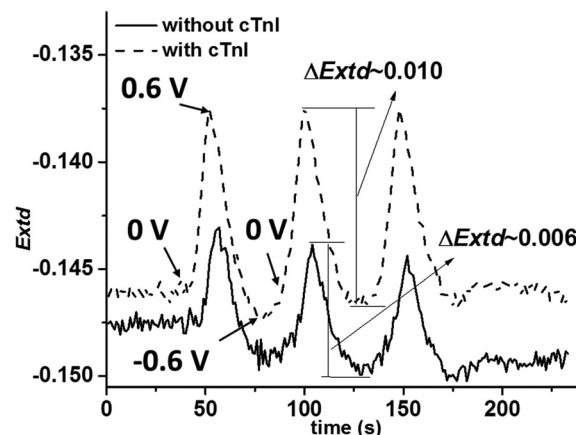

Fig. 2 LSPR responses of the modified AuNH array under voltage sweeping measured in PBS buffer before (solid line) and after incubation of 3 μg mL^{-1} cTnI for 30 min (dashed line). The voltage was swept (three cycles) from 0 V, 0.6 V, −0.6 V and back to 0 V at a scanning rate of 100 mV s^{-1}.

the center of a chip. The AuNH array was characterized by scanning electron microscopy (SEM), atomic force microscopy (AFM) and UV-vis spectroscopy (UV-vis) (Fig. 1), all indicating a periodic and uniform hole array. The plasmon resonance peak typically shifts to a higher wavelength upon molecular binding to the surface of the nanohole, leading to a decrease of the extinction difference Extd (Fig. 1d). The Extd was obtained from the extinction intensity difference at two wavelengths, *e.g.* λ_1 and λ_2 (Fig. 1d). The AuNH array was modified in a 1 : 1 mixture of a short peptide CALNN and CALNN-(PEG)$_4$-FYSHSFHENWPS,[45] a peptide specific for cTnI (see the details in the ESI†). Extinction spectra were measured by using an Xnano instrument (Insploroion) and the Extd between two pre-selected wavelengths at about λ_1 = 700 nm and λ_2 = 730 nm was monitored in real-time (*i.e.* Extd(t) = Ext$_{730}$(t) − Ext$_{700}$(t)).

In order to investigate the effect of applied electric bias on LSPR response, three cycles of voltage scans (from 0 V, 0.6 V, −0.6 V and back to 0 V at a scanning rate of 100 mV s^{-1} *vs.* the Ag/AgCl electrode) were applied on the peptide-modified AuNH array before and after incubation with cTnI in the PBS

buffer (Fig. 2). The Extd value shifted synchronously with the applied bias. Positive bias resulted in an increasing Extd value (less negative), indicating red-shift of the LSPR peak, while negative bias induced a blue-shift (Fig. S1†). The relative magnitude of the observed shifts is attributed to the higher polarizability of the Cl$^-$ ion (4.17 Å^3) with respect to water molecules (1.43 Å^3) and Na$^+$ ions (0.148 Å^3).[46] According to the DLVO theory, the applied electric field on the surface influences the electric double layer in solution. The different strength of the applied potential results in a redistribution of ions within the double layer, thus varying the refractive index near the surface.[47] Interestingly, the chip after binding with cTnI showed higher Extd changes (ΔExtd) under voltage sweeping from 0.6 V to −0.6 V (Fig. 2). This is most likely due to an increase in the effective surface area of the AuNH after the binding of positively charged cTnI molecules (see the AFM imaging in Fig. S2†), resulting indirectly in an increasing concentration of highly polarizable Cl$^-$ ions near the surface.

Real-time measurements of the LSPR response upon injection of cTnI (PBS) into the reaction chamber were carried out under different biases applied to the sensor chip (*vs.* the Ag/AgCl electrode), as shown in Fig. 3a. The ΔExtd (with the background Extd offset to zero) slowly increased after the injection of 100 ng mL^{-1} cTnI under 0 V bias and the response increased with the concentration of cTnI beyond 100 ng mL^{-1}. The control experiment carried out on the sensor chip without the specific peptide modification (only CALNN) revealed negligible nonspecific adsorption (Fig. S3†). The ΔExtd value of each concentration was calculated by subtracting the background value (ΔExtd(t < 60 min)) from that after 30 min incubation. The calibration curve under 0 V (triangles in Fig. 3b) was fitted by a sigmoidal model (eqn S1†), and the LOD was estimated to be ~110 ng mL^{-1} for our platform under 0 V. The noise level was calculated as 3 times the standard deviation of the Extd before injection of cTnI in the solution.
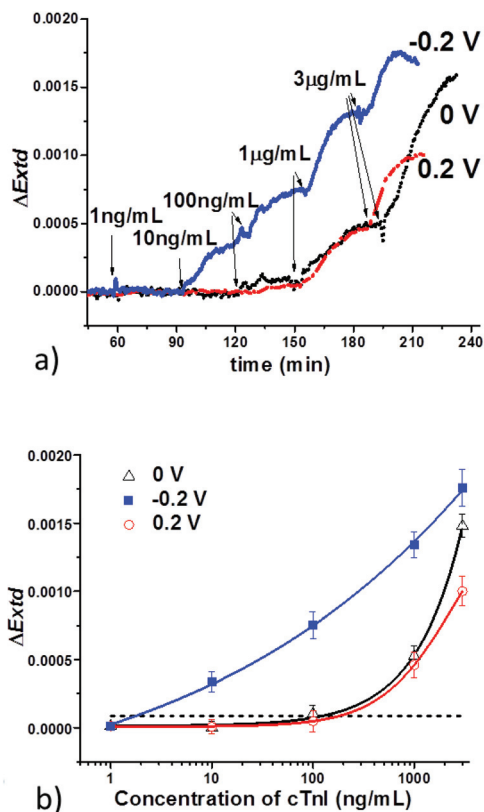
Fig. 3 (a) Real-time ΔExtd measured on the AuNH array with a series of injections of cTnI in PBS. Sensor response for 0 V (black curve), −0.2 V (blue curve) and 0.2 V (red curve). (b) Extd changes (ΔExtd) as a function of the cTnI concentration measured under no bias (triangles), −0.2 V bias (squares) and 0.2 V bias (circles). Dotted line is 3 times standard deviation.

Table 1 Result of cTnI assay using AuNH as sensor under different biases

Medium	Bias (V)	LOD (ng mL^{-1})
PBS	0	110
PBS	0.2	170
PBS	−0.2	1.8
BSA	−0.2	8^a
Serum	−0.2	25^b

^{a} With 3 mg mL^{-1} BSA in PBS. ^{b} In 10× diluted rabbit serum in PBS.

While, the negatively charged molecules such as BSA (pI = 4.7) are repelled from the sensor surface the nonspecific adsorption is expected to decrease. For instance, after injection of 3 mg mL^{-1} BSA into PBS, the LSPR sensor response due to BSA adsorption decreased by a factor of 2 at −0.2 V bias (Fig. S4†). To investigate the possibility of detecting cTnI in complex samples at −0.2 V bias, we started by adding various concentrations of cTnI (1 ng mL^{-1} to 3 μg mL^{-1}) in PBS containing 3 mg mL^{-1} BSA. The extinction changes were monitored in real time before and after the injection of the cTnI in the BSA containing buffer solutions (Fig. 4a). A slow increase of the ΔExtd was seen upon the injection of 3 mg mL^{-1} BSA.
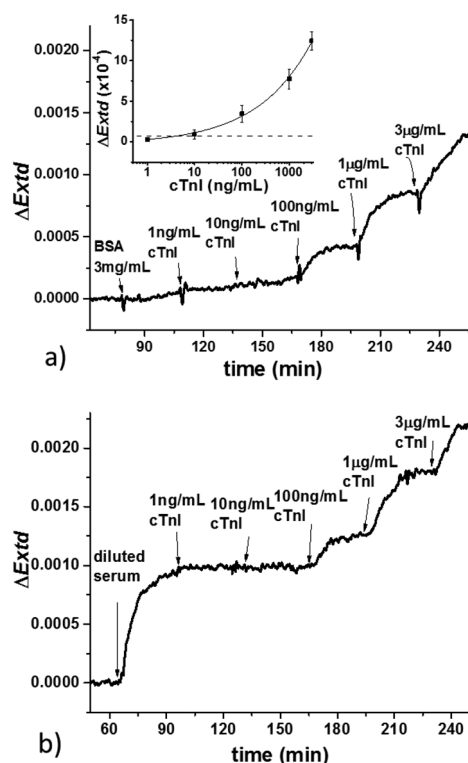
Assuming the binding events are limited by the mass transport diffusion, the surface coverage of molecules on the sensor surface during the incubation time of t can be simplified as $\Gamma = 2C_{bulk}\sqrt{Dt/\pi}$,[33,48,49] where C_{bulk} is the bulk concentration of analyte in the solution, D is the diffusion constant of the molecules (see details in the ESI†). Based on an LOD of 110 ng mL^{-1} achieved for 30 min incubation (0 V), we are able to estimate the smallest detectable surface mass of Γ_{LOD} = 2.9 ng cm^{-2}. Thus our results indicate that it is necessary to allow for 63 days of incubation to achieve an LOD of 2 ng mL^{-1}, which is approximately the clinical level of cTnI found in healthy people.

The binding rate and the sensor response were significantly improved under −0.2 V bias applied to the sensor chip. For instance, the initial binding rate for 10 ng mL^{-1} cTnI is comparable to 1 μg mL^{-1} cTnI under 0 V bias. The LOD is improved by two orders of magnitude to 1.8 ng mL^{-1} under −0.2 V bias (Fig. 3b, Table 1), for a reaction time of 30 min, which is theoretically more than 3000 times faster than the diffusion limited assay $t \sim$ 77.5 days at 0 V. Positive bias applied on the sensor surface hinders the binding of cTnI to the sensor surface, thereby worsening the LOD to 170 ng mL^{-1} (Fig. 3, Table 1).

Fig. 4 (a) Real-time LSPR signals of AuNH array under −0.2 V bias. Inset is the calibration curve for the detection of cTnI spiked in PBS with 3 mg ml^{-1} BSA under −0.2 V bias. (b) The real-time Extd changes measured on the AuNH array under −0.2 V bias for the detection of cTnI in 10× diluted rabbit serum.

Sequential injections of cTnI revealed a significant response at 100 ng mL^{-1} cTnI, and a LOD of about 8 ng mL^{-1} was estimated for the detection of cTnI in 3 mg mL^{-1} BSA, see insert Fig. 4a and Table 1. This result indicated the feasibility for the detection of cTnI in a solution of high BSA concentration, and potentially also for more complex biofluids like serum or plasma.

The nonspecific adsorption of a 10-time diluted rabbit serum was subsequently investigated (Fig. 4b). The nonspecific adsorption was reduced by a factor of 2 by monitoring the ΔExtd after applying −0.2 V bias (Fig. S5†). However, the response induced by the nonspecific adsorption (ΔExtd = 0.001) was still higher than the specific sensor response to 3 μg mL^{-1} cTnI (Fig. 4b), suggesting that other molecules/proteins than serum albumin (e.g. globulins and antibodies) may adsorb to the sensor surface. In serum, the major protein is serum albumin with a concentration of 35–52 mg mL^{-1}. Other proteins include globulins (22–40 mg mL^{-1}, isoelectric point, pI ∼ 7.5), antibodies (total 5.8–27 mg mL^{-1}) and many more at lower concentration.[50] Due to their high concentration and weakly positive charge, nonspecific adsorption induced by globulins, and to some extent also by antibodies, were unavoidable under −0.2 V bias. Nevertheless, the sensor response to cTnI at 100 ng mL^{-1} was comparable to that measured in PBS buffer. A LOD of 25 ng mL^{-1} was achieved in serum samples (Fig. S6†). Control experiments carried out under bias of 0.4 V and −0.4 V indicated the poor long-term stability of the sensor response, which might be ascribed to the dissociation of the thiol molecules from the sensor surface and/or oxidation/chlorination of the gold film. Taken together, electro-focusing at −0.2 V offers a route to reduce non-specific adsorption of negatively charged proteins to the peptide modified AuNH array thereby allowing for the detection of cTnI in biofluids of increasing complexity.

Conclusions

We have successfully demonstrated an electrofocusing-enhanced plasmonic sensor based on a gold nanohole array for the detection of cTnI in buffer, BSA solution and rabbit serum. The limit of detection (LOD) in buffer can be improved by ∼2 orders of magnitude upon changing from 0 to −0.2 V bias applied to the sensor surface. The nonspecific adsorption of serum albumin (i.e. BSA) and rabbit serum is also reduced at −0.2 V. This method provides an avenue for highly sensitive detection of biomolecules in complex fluids like serum without tedious sample purification and pretreatment.

Acknowledgements

Notes and references

1 E. Altewischer, M. P. van Exter and J. P. Woerdman, Nature, 2002, 418, 304–306.
2 S. Linic, P. Christopher and D. B. Ingram, Nat. Mater., 2011, 10, 911–921.
3 S. C. Warren and E. Thimsen, Energy Environ. Sci., 2012, 5, 5133–5146.
4 X. Huang, Y. Li, Y. Chen, H. Zhou, X. Duan and Y. Huang, Angew. Chem., Int. Ed., 2013, 52, 6063–6067.
5 Q. Gan, F. J. Bartoli and Z. H. Kafafi, Adv. Mater., 2013, 25, 2385–2396.
6 J. Homola, Chem. Rev., 2008, 108, 462–493.
7 X. Liu, Y. Wang, P. Chen, Y. Wang, J. Mang, D. Aili and B. Liedberg, Anal. Chem., 2014, 86, 2345–2352.
8 Y. Wang, X. Liu, J. Zhang, D. Aili and B. Liedberg, Chem. Sci., 2014, 5, 2651–2656.
9 L. J. Sherry, S. H. Chang, G. C. Schatz, R. P. Van Duyne, B. J. Wiley and Y. N. Xia, Nano Lett., 2005, 5, 2034–2038.
10 G. Raschke, S. Kowarik, T. Franzl, C. Sonnichsen, T. A. Klar, J. Feldmann, A. Nichtl and K. Kurzinger, Nano Lett., 2003, 3, 935–938.
11 K. M. Mayer and J. H. Hafner, Chem. Rev., 2011, 111, 3828–3857.
12 A. Kinkhabwala, Z. Yu, S. Fan, Y. Avlasevich, K. Muellen and W. E. Moerner, Nat. Photonics, 2009, 3, 654–657.
13 J. R. Lakowicz, K. Ray, M. Chowdhury, H. Szmacinski, Y. Fu, J. Zhang and K. Nowaczyk, Analyst, 2008, 133, 1308–1346.
14 D. Punj, M. Mivelle, S. B. Moparthi, T. S. van Zanten, H. Rigneault, N. F. van Hulst, M. F. Garcia-Parajo and J. Wenger, Nat. Nanotechnol., 2013, 8, 512–516.
15 Y. Wang, A. Brunsen, U. Jonas, J. Dostalek and W. Knoll, Anal. Chem., 2009, 81, 9625–9632.
16 Y. Wang, J. Dostalek and W. Knoll, Biosens. Bioelectron., 2009, 24, 2264–2267.
17 M. D. Porter, R. J. Lipert, L. M. Siperko, G. Wang and R. Narayanana, Chem. Soc. Rev., 2008, 37, 1001–1011.
18 P. Chen, Z. Yin, X. Huang, S. Wu, B. Liedberg and H. Zhang, J. Phys. Chem. C, 2011, 115, 24080–24084.
19 Y. Zhang, J. Qian, D. Wang, Y. Wang and S. He, Angew. Chem., Int. Ed., 2013, 52, 1148–1151.
20 S. Schluecker, Angew. Chem., Int. Ed., 2014, 53, 4756–4795.
21 M. Frasconi, C. Tortolini, F. Botre and F. Mazzei, Anal. Chem., 2010, 82, 7335–7342.
22 L. He, M. D. Musick, S. R. Nicewarner, F. G. Salinas, S. J. Benkovic, M. J. Natan and C. D. Keating, J. Am. Chem. Soc., 2000, 122, 9071–9077.
23 S. Krishnan, V. Mani, D. Wasalathanthri, C. V. Kumar and J. F. Rusling, Angew. Chem., Int. Ed., 2011, 50, 1175–1178.
24 A. W. Wark, H. J. Lee, A. J. Qavi and R. M. Corn, Anal. Chem., 2007, 79, 6697–6701.
25 T. T. Goodrich, H. J. Lee and R. M. Corn, J. Am. Chem. Soc., 2004, 126, 4086–4087.

26 H. J. Lee, Y. Li, A. W. Wark and R. M. Corn, *Anal. Chem.*, 2005, **77**, 5096–5100.

27 H. M. Lou, J. Y. Zhu, T. Q. Lan, H. R. Lai and X. Q. Qiu, *ChemSusChem*, 2013, **6**, 919–927.

28 Y. Wang, J. Dostalek and W. Knoll, *Anal. Chem.*, 2011, **83**, 6202–6207.

29 Y. Wang, W. Knoll and J. Dostalek, *Anal. Chem.*, 2012, **84**, 8345–8350.

30 E. C. Lin, J. Fang, S. C. Park, F. W. Johnson and H. O. Jacobs, *Nat. Commun.*, 2013, 4.

31 E.-C. Lin, J. Fang, S.-C. Park, T. Stauden, J. Pezoldt and H. O. Jacobs, *Adv. Mater.*, 2013, **25**, 3554–3559.

32 D. Pallarola, M. Schneckenburger, J. P. Spatz and C. Pacholski, *Chem. Commun.*, 2013, **49**, 8326–8328.

33 A. Barik, L. M. Otto, D. Yoo, J. Jose, T. W. Johnson and S.-H. Oh, *Nano Lett.*, 2014, **14**, 2006–2012.

34 A. B. Dahlin, T. Sannomiya, R. Zahn, G. A. Sotiriou and J. Voeroes, *Nano Lett.*, 2011, **11**, 1337–1343.

35 K. J. Foley, X. Shan and N. J. Tao, *Anal. Chem.*, 2008, **80**, 5146–5151.

36 C. Novo and P. Mulvaney, *Nano Lett.*, 2007, **7**, 520–524.

37 T. Sannomiya, H. Dermutz, C. Hafner, J. Voeroes and A. B. Dahlin, *Langmuir*, 2010, **26**, 7619–7626.

38 X. Shan, U. Patel, S. Wang, R. Iglesias and N. Tao, *Science*, 2010, **327**, 1363–1366.

39 S. Wang, X. Huang, X. Shan, K. J. Foley and N. Tao, *Anal. Chem.*, 2010, **82**, 935–941.

40 X. R. Cheng, B. Y. H. Hau, T. Endo and K. Kerman, *Biosens. Bioelectron.*, 2014, **53**, 513–518.

41 T. G. Drummond, M. G. Hill and J. K. Barton, *Nat. Biotechnol.*, 2003, **21**, 1192–1199.

42 T. Sannomiya, O. Scholder, K. Jefimovs, C. Hafner and A. B. Dahlin, *Small*, 2011, **7**, 1653–1663.

43 Y. Wang, L. Wu, X. D. Zhou, T. I. Wong, J. L. Zhang, P. Bai, E. P. Li and B. Liedberg, *Sens. Actuators, B*, 2013, **186**, 205–211.

44 T. I. Wong, S. Han, L. Wu, Y. Wang, J. Deng, C. Y. L. Tan, P. Bai, Y. C. Loke, X. D. Yang, M. S. Tse, S. H. Ng and X. Zhou, *Lab Chip*, 2013, **13**, 2405–2413.

45 J. P. Park, D. M. Cropek and S. Banta, *Biotechnol. Bioeng.*, 2010, **105**, 678–686.

46 E. A. Mason and E. W. McDaniel, in *Transport Properties of Ions in Gases*, Wiley-VCH Verlag GmbH & Co. KGaA, 2005, pp. 531–539.

47 A. B. Dahlin, B. Dielacher, P. Rajendran, K. Sugihara, T. Sannomiya, M. Zenobi-Wong and J. Voros, *Anal. Bioanal. Chem.*, 2012, **402**, 1773–1784.

48 D. B. Hibbert, J. J. Gooding and P. Erokhin, *Langmuir*, 2002, **18**, 1770–1776.

49 A. B. Dahlin, *Plasmonic biosensors: an integrated view of refractometric detection*, Ios Press, 2012.

50 D. Weatherby and S. Ferguson, *Blood chemistry and cbc analysis: clinical laboratory testing from a functional perspective*, Vis Medicatrix Press, Jacksonville, OR, 2004.